Electron Capture/Negative Ionization Mass Spectrometric Characteristics of Bioaccumulating Methyl Sulfone-Substituted Polychlorinated Biphenyls

Robert J. Letcher[1] and Ross J. Norstrom[1,2]*

[1] Centre for Analytical and Environmental Chemistry, Department of Chemistry, Carleton University, Ottawa, Ontario, K1S 5B6, Canada

[2] Environment Canada, Canadian Wildlife Service, Hull, Québec, K1A 0H3, Canada

Gas chromatography/electron-capture negative ionization mass spectrometry (GC/ECNI-MS) was used to separate and detect a mixture of 24, 3-and 4-methyl sulfone-substituted polychlorinated biphenyls ($MeSO_2$-PCBs). The dominant fragment ions were $[M - CH_3]^-$ and $[M - Cl + H]^-$, and to a lesser extent $[M - 2Cl]^-$, $[M - 2Cl + 2H]^-$, $[M - CH_3\text{-}Cl + H]^-$ and $[M - SO_2CH_3 + H]^-$). The structures of the 3-and 4-$MeSO_2$-PCBs varied in the degree (i.e. tetrachloro-to heptachloro-) and position of chlorine substitution. With the assistance of multivariate statistical analysis, the abundance of several isotopic clusters of fragment ions relative to that of the molecular ion (M^-) was found to vary as a function of $MeSO_2$-PCB structure. Compared with other congeners, the relative abundance of $[M - CH_3]^-$ was significantly lower for $MeSO_2$-PCBs containing the 4-$MeSO_2$-2,5-dichloro moiety, and the hexachloro-and heptachloro-$MeSO_2$-PCBs had higher relative abundances of $[M - Cl + H]^-$. Subtle ECNI mass spectral fragmentation rules therefore exist for 3-and 4-$MeSO_2$-PCBs with respect to congener structure; however, both ion source temperature and pressure must be controlled. Increasing the ion source temperature from 100 to 260 °C resulted in an large increase in the abundance of $[M - CH_3]^-$ relative to M^- from <20% to >100%, for all the $MeSO_2$-PCBs studied. For the set of ten 3-/4-$MeSO_2$-PCB pairs, the $[M - CH_3]^-$ relative abundance ratio was independent of ion source temperature, and was ~4.5 and ~1.5 for congeners possessing 2,5-dichloro and 2,5,6-trichloro substitution on the $MeSO_2$-containing phenyl ring, respectively. The effect of an increase in ion source temperature, over the same temperature range, on the relative abundance of hydrogen inclusion-type fragment ions was much less dramatic. $[M - CH_3\text{-}Cl + H]^-$ and $[M - Cl + H]^-$ abundance often increased, but never exceeded ~40%. Decreasing the methane reagent gas pressure from 0.5 to 0.05 mbar did not significantly alter the ion source temperature effect on the relative abundance of the fragment ions. However, the ECNI response sensitivity decreased by an order of magnitude. © 1997 by John Wiley & Sons, Ltd.

INTRODUCTION

Electron-capture negative ionization mass spectrometry (ECNI-MS) has proven to be a sensitive technique for the detection of electrophilic compounds, which is made possible by the introduction of a reagent gas such as methane in the ion source.[1–3] The reagent gas used in ECNI facilitates the "thermalization" of high-energy electrons emitted from the ion source filament by inelastic scattering and dissociative ionization processes.[4] The quasi-thermal electrons (i.e. 0–15 eV) are sufficiently de-energized to be captured by the analyte. Negative ion mass spectra result from three ion-forming processes: (i) ion-pair formation, (ii) electron attachment and (iii) dissociative electron attachment.[4–7] Electron attachment to form a vibrationally excited molecular radical anion (M^-*) can subsequently undergo a resonance stabilizing process. Collisional deactivation accompanied by radiation emission produces a molecular ion (i.e. $M^{-\cdot}$, or written as M^-) from M^-*, if the electron affinity of the analyte is positive (i.e. >0) permitting a sufficiently long-lived M^-* relative to autodetachment of the captured electron.[4,7] For analytes with electron affinities <0, a Frank–Condon transition, with respect to potential energy surfaces for negative ion formation, can lead to an unstable M^-* which can undergo a dissociative resonance process. Alternately, dissociation of $M^{-\cdot}$ to form a radical and an anionic species occurs if a repulsive state of $M^{-\cdot}$ is generated as a consequence of a vertical Frank–Condon transition.

Secondary processes in ECNI mass spectra are known to occur such as electron capture by a species generated by heterogeneously catalyzed hydrogenation or chlorination of the analyte on surfaces of the ion source.[2,7,8] Ion–molecule reactions can also occur

* Correspondence to: R. J. Norstrom, Environment Canada, Canadian Wildlife Service, National Wildlife Research Centre, 100 Gamelin Blvd., Hull, Québec, K1A 0H3 Canada.

between the analyte and radical anion forms of a reactive reagent gas such as oxygen, and/or reaction of the radical analyte anion with oxygen.[3,5]

Methyl sulfone-substituted polychlorinated biphenyl (MeSO$_2$-PCB) compounds are responsive to ECNI-MS.[9,10] The 3- and 4-MeSO$_2$-PCBs (Fig. 1) are a class of environmental contaminants known to persist and bioaccumulate in the tissues of living organisms, and have potential toxicological significance.[11–16] The MeSO$_2$-PCBs are metabolites that result from the enzyme-mediated biotransformation of PCB congeners that are not substituted at one of the *meta–para* positions.[17–19] Gas chromatography (GC)/ECNI-MS analysis using methane as a reagent gas has been shown to be approximately 500 times more sensitive than GC/ EI-MS (electron impact) towards MeSO$_2$-PCB compounds, and useful for identifying isomeric MeSO$_2$-PCBs based on the degree of chlorination. Further structural characterization from either the EI or ECNI mass spectral fragmentation pattern has been limited to differences in 2-MeSO$_2$-and 2'-Cl-substituted MeSO$_2$-PCBs from other MeSO$_2$-PCB structures.[9,10,20,21] A recent attempt to differentiate MeSO$_2$-PCBs based on the structure–ECNI-MS fragmentation relationships derived from the mass spectra of 94 congeners was complicated by ion–molecule reactions between oxygen and the MeSO$_2$-PCB analytes.[10] In the present study, the ECNI mass spectra and the effect of congener structure on the ECNI-MS fragmentation of 24, 3- and 4-MeSO$_2$-PCBs in an oxygen-free GC/ECNI-MS system were examined. Additional MeSO$_2$-PCB structural information may be derived from the abundance of fragment ions relative to M$^-$. Possible rules may be derived from the quantitative differences in fragment ion abundance which would be useful in the identification of 3- and 4-MeSO$_2$-PCBs in biological samples and synthetic products containing isomeric 3- and 4-MeSO$_2$-PCBs.

The abundance of anions originating from the ECNI ion-forming processes are dependent on, among other factors, the sample amount, the type and pressure of the reagent gas, ionizing electron energy and current, the ion source temperature and physical parameters of the MS instrument.[2] The effects of changes in ion source temperature and the pressure of the methane reagent

gas on the ECNI mass spectra of MeSO$_2$-PCBs were examined.

EXPERIMENTAL

Chemicals and standards

The 24 individual MeSO$_2$-PCB standards used in this study were synthesized by Dr. Åke Bergman (Wallenberg Laboratory, Stockholm University, Stockholm, Sweden) and Dr. K. Haraguchi (Daiichi Pharmaceutical College, Fukuoka, Japan).[10,20] Two mixtures of the MeSO$_2$-PCB standards, one containing 16 and the other 12 congeners, were prepared in 2,2,4-trimethylpentane (BDH, analytical grade) at a concentration of ~ 250 pg ml^{-1}. Six of the MeSO$_2$-PCB congener standards were present in both mixtures to monitor potential changes in the fragmentation pattern between separate GC/ECNI-MS injections. The difference in the abundance of the MeSO$_2$-PCB fragment ions among replicates ($n = 2$) was quantitatively insignificant (i.e. $<1\%$). Two separate mixtures were necessary to prevent co-elution of individual congeners under the GC column and temperature ramping conditions used.

GC/ECNI-MS analysis

The MeSO$_2$-PCB standard mixtures were analyzed by GC/ECNI-MS (TIC), scanned from 80 to 550 amu to ensure detection of all molecular and predominant fragment anions. The sum of the ion abundances in each isotopic cluster was used to determine the abundance of the fragment ions relative to the M$^-$ base peak (Table 1). Haraguchi *et al.*[10] and Buser *et al.*[9] compared the relative abundances of molecular and fragment ions of MeSO$_2$-PCBs based on monoisotopic ^{35}Cl ions in each isotopic cluster. Comparing fragment ion abundances among MeSO$_2$-PCBs based on a single isotopic peak is biased since the relative abundance of the isotopic ions in the cluster varies depending on the number of chlorines present in the fragment and in the congener. The ECNI mass spectrum for each MeSO$_2$-PCB congener was taken from a single scan at the maximum of the corresponding GC peak.

Ion source conditions were optimized for production of a plasma of thermalized secondary electrons generated from methane reaction gas,[22] and based on the GC/ECNI-MS conditions for the determination of MeSO$_2$-PCBs in polar bear tissues from the Canadian Arctic.[13–15] An ion source temperature of 140 °C and pressure of 0.5 mbar (1 bar = 10^5 Pa) was chosen to compare the abundance of the fragment ions relative to M$^-$. The emission current was 300 µA and the primary electron beam energy was 130 eV. A gas pressure of ~ 0.3–0.6 mbar, a temperature of 140–200 °C and a primary electron beam energy of 35–150 eV in the ion source have been found to give optimal electron-capture enhancement of polyhalogenated aromatic hydrocarbons, including PCBs.[22] The injection port and transfer line temperatures were 270 and 280 °C, respectively. The instrument was tuned with perfluorotributylamine (PFTBA) using m/z 312, 414 and 464. The effect of

X = 1 - 4

X = 1 - 3
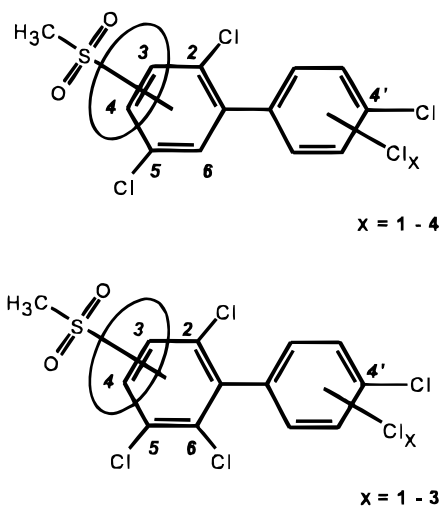
Figure 1. Structures of MeSO$_2$-PCBs that persist in biota. Hydrogens on the phenyl rings have been omitted for clarity.

Table 1. Relative percentage abundances of MeSO$_2$-PCB fragment ions with respect to the molecular ion base peak using GC/ECNI-MS^a

No.	Congener	Cl substitution^b	[M − CH$_3$]$^-$ [M − 15]$^-$	[M − Cl + H]$^-$ [M − 34]$^-$	[M − CH$_3$ − Cl + H]$^-$ [M − 49]$^-$	[M − 2Cl + 2H]$^-$ [M − 68]$^-$	[M − 2Cl]$^-$ [M − 70]$^-$	[M − SO$_2$CH$_3$ + H]$^-$ [M − 78]$^-$
1	3-MeSO$_2$-CB49	2,2′,4′,5	16	5	2	<1	<1	<1
2	4-MeSO$_2$-CB49	2,2′,4′,5	8	7	1	<1	<1	<1
3	3-MeSO$_2$-CB70	2,3′,4′,5	10	12	6	1	<1	<1
4	4-MeSO$_2$-CB70	2,3′,4′,5	3	10	1	<1	1	<1
5	3-MeSO$_2$-CB52	2,2′,5,5′	18	9	1	<1	<1	<1
6	4-MeSO$_2$-CB52	2,2′,5,5′	5	6	<1	<1	<1	<1
7	4-MeSO$_2$-CB64	2,4′,5,6	21	8	1	1	1	<1
8	3-MeSO$_2$-CB110	2,3′,4′,5,6	16	13	2	2	2	1
9	4-MeSO$_2$-CB110	2,3′,4′,5,6	14	12	2	2	3	<1
10	3-MeSO$_2$-CB101	2,2′,4′,5,5′	14	10	2	2	2	1
11	4-MeSO$_2$-CB101	2,2′,4′,5,5′	4	8	1	1	2	1
12	3-MeSO$_2$-CB87	2,2′,3′,4′,5	18	14	3	2	3	2
13	4-MeSO$_2$-CB87	2,2′,3′,4′,5	5	13	2	2	2	<1
14	3-MeSO$_2$-CB91	2,2′,4′,5,6	22	14	3	2	2	<1
15	4-MeSO$_2$-CB95	2,2′,5,5′,6	14	10	1	1	1	<1
16	3-MeSO$_2$-CB149	2,2′,4′,5,5′,6	19	16	3	3	3	2
17	4-MeSO$_2$-CB149	2,2′,4′,5,5′,6	15	24	2	7	6	2
18	3-MeSO$_2$-CB132	2,2′,3′,4′,5,6	16	14	2	3	3	1
19	4-MeSO$_2$-CB132	2,2′,3′,4′,5,6	14	15	2	4	3	1
20	3-MeSO$_2$-CB141	2,2′,3′,4′,5,5′	14	18	3	4	4	12
21	4-MeSO$_2$-CB141	2,2′,3′,4′,5,5′	3	14	<1	2	2	10
22	4-MeSO$_2$-CB151	2,2′,3′,5,5′,6′	15	10	2	2	1	3
23	3-MeSO$_2$-CB174	2,2′,3′,4′,5,5′,6	12	16	2	4	5	8
24	4-MeSO$_2$-CB174	2,2′,3′,4′,5,5′,6	7	22	1	4	3	9

^{a} The abundance of each ion is based on the cumulative response all the ions in the isotopic cluster. The molecular ion was consistently the base peak (ion source temperature and pressure 140 °C and 0.5 mbar, respectively) and given a relative abundance of 100%. The values are the average of $n = 2$ replicate analyses.
^{b} See Fig. 1 for the positions of the MeSO$_2$ − and chlorine-group substitutions on the biphenyl system.

changing the ion source temperature from 100 to 260 °C in increments of 20 °C on the ECNI mass spectral fragmentation pattern of the 24 MeSO$_2$-PCBs (Table 1) was tested at two ion source pressures, 0.5 and 0.05 mbar.

GC/ECNI-MS was performed on an HP 5987B mass spectrometer upgraded with an HP 5890 Series II gas chromatograph coupled with an HP 5988 GC/MS direct interface. The ECNI-MS system was fitted with stainless-steel lines, fittings and other internal components, under the supervision of Professor Dr. M. Oehme (Institute for Organic Chemistry, University of Basel, Basel, Switzerland), to minimize ion source contamination by reactive, synthetic components. Leakage of atmospheric gases, including oxygen, was also minimized as a consequence of the air-tight construction of the GC/ECNI-MS system. The GC carrier and ion source reagent gas were helium (99.99%) and methane (99.99%), respectively. The GC/ECNI-MS was fitted with a fused-silica Rtx-5 capillary column (Restek, Bellefonte, PA, USA) of 30 m × 0.25 MM i.d., with a 0.1 µm film thickness of cross-linked 95% dimethyl–5% diphenylpolysiloxane. All injections were 2 µl in volume and made in the splitless mode. The GC oven temperature program was as follows: initial temperature held at 100 °C for 3 min, then increased at 20 °C min^{-1} to 220 °C and at 3 °C min^{-1} to 280 °C.
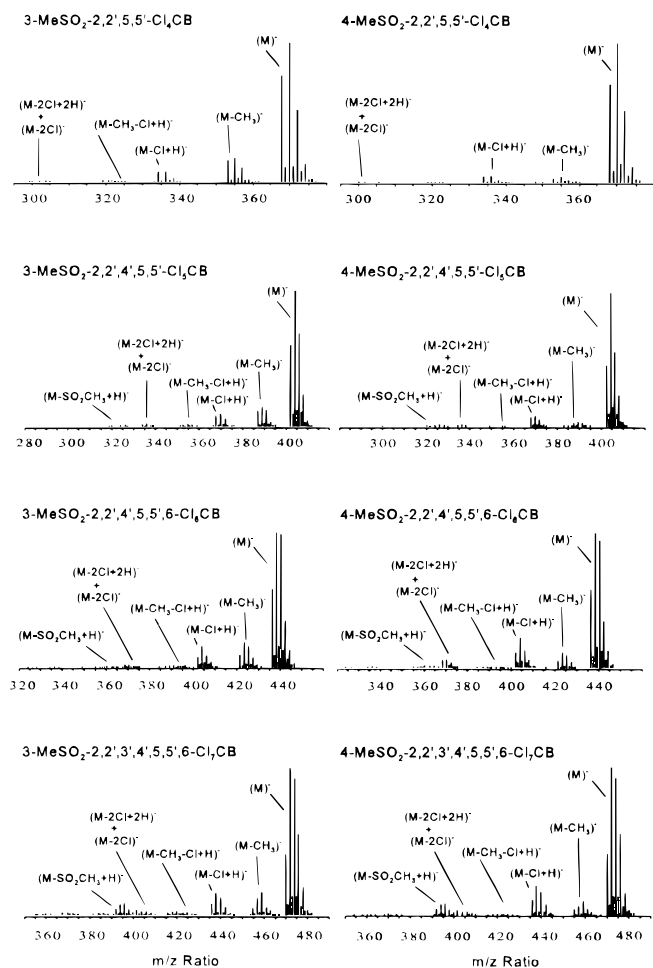
Statistical analysis

Subtle differences in the relative abundance of the major fragment anions among the MeSO$_2$-PCB congeners

warranted the use of a multivariate statistical approach to the analysis. Principal component analysis (PCA) was chosen using the Pirouette (version 1.2) software package (Infometrix, Seattle, WA, USA). PCA analysis was useful in modelling the overall variation to observe more clearly MeSO$_2$-PCB structural factors that may be contributing to changes in the relative abundance of the ECNI-MS-generated fragment anions. PCA transforms a complex data set into a new set of variables, known as eigenvectors or principal components (PC), that are linear combinations of the original variables in the data set. The magnitude of a PC determines how much of the data variation it contains. A favourable PCA analysis should explain a large proportion of the variation in the first two or three PCs. The PCA was not auto-scaled to permit the variations of the largest fragment ion abundances to be the most influential on the PCs. Score and loading plots for PC1 versus PC2 were generated to demonstrate the spatial relationships among MeSO$_2$-PCB congeners and how each fragment ion influenced the direction of the PC, respectively.

RESULTS AND DISCUSSION

ECNI mass spectra of MeSO$_2$-PCBs

The MeSO$_2$-PCB mass spectra in Fig. 2 illustrate the absence of significant amounts of oxygen in the present GC/ECNI-MS system. The [M − Cl + O]$^-$ fragment ion was either not measurable or <1% of the M$^-$ base

3-MeSO$_2$-2,2',5,5'-Cl$_4$CB

(M)˙

(M-2Cl+2H)˙
(M-2Cl)˙ (M-CH$_3$-Cl+H)˙ (M-CH$_3$)˙
(M-Cl+H)˙

300 320 340 360

4-MeSO$_2$-2,2',5,5'-Cl$_4$CB

(M)˙

(M-2Cl+2H)˙
(M-2Cl)˙
(M-Cl+H)˙ (M-CH$_3$)˙

300 320 340 360

3-MeSO$_2$-2,2',4',5,5'-Cl$_5$CB

(M)˙

(M-2Cl+2H)˙
(M-2Cl)˙ (M-CH$_3$)˙
(M-SO$_2$CH$_3$+H)˙ (M-CH$_3$-Cl+H)˙
(M-Cl+H)˙

280 300 320 340 360 380 400

4-MeSO$_2$-2,2',4',5,5'-Cl$_5$CB

(M)˙

(M-2Cl+2H)˙
(M-2Cl)˙ (M-CH$_3$)˙
(M-SO$_2$CH$_3$+H)˙ (M-CH$_3$-Cl+H)˙
(M-Cl+H)˙

300 320 340 360 380 400

3-MeSO$_2$-2,2',4',5,5',6-Cl$_6$CB

(M)˙

(M-2Cl+2H)˙
(M-2Cl)˙ (M-CH$_3$-Cl+H)˙ (M-CH$_3$)˙
(M-SO$_2$CH$_3$+H)˙ (M-Cl+H)˙

320 340 360 380 400 420 440

4-MeSO$_2$-2,2',4',5,5',6-Cl$_6$CB

(M)˙

(M-2Cl+2H)˙
(M-2Cl)˙ (M-CH$_3$)˙
(M-CH$_3$-Cl+H)˙
(M-SO$_2$CH$_3$+H)˙ (M-Cl+H)˙

340 360 380 400 420 440

3-MeSO$_2$-2,2',3',4',5,5',6-Cl$_7$CB

(M)˙

(M-2Cl+2H)˙
(M-2Cl)˙ (M-CH$_3$-Cl+H)˙ (M-CH$_3$)˙
(M-SO$_2$CH$_3$+H)˙ (M-Cl+H)˙

360 380 400 420 440 460 480

m/z Ratio

4-MeSO$_2$-2,2',3',4',5,5',6-Cl$_7$CB

(M)˙

(M-2Cl+2H)˙
(M-2Cl)˙ (M-CH$_3$)˙
(M-CH$_3$-Cl+H)˙
(M-SO$_2$CH$_3$+H)˙ (M-Cl+H)˙

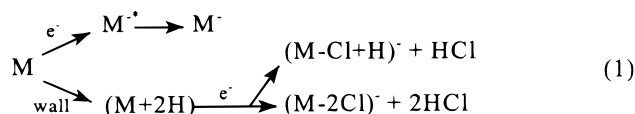360 380 400 420 440 460 480

m/z Ratio

Figure 2. ECNI mass spectra of tetrachloro-to heptachloro-, 3- and 4-MeSO$_2$-PCBs. See Fig. 1 for the congener structure. The major fragment ions are labeled.
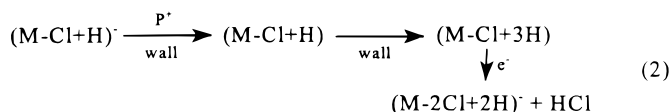
peak. In a previous GC-ECNI-MS analysis of 94 MeSO$_2$-PCBs by Haraguchi *et al.*,[10] the [M − Cl + O]$^-$ ion was generally the most intense peak in the mass spectra despite the use of methane buffer gas containing <100 ppm O$_2$. As a consequence, potential relationships between MeSO$_2$-PCB structure and the relative abundance of fragment ions not containing oxygen were obscured. Minute leakage of oxygen from surrounding air into the ECNI-MS ion source is known to result in reactions with halogenated analytes producing the [M − X + O]$^-$ species (i.e. X = Cl or Br). For example, PCBs[23,24] and polycyclic chlorinated pesticides[8] produce [M − Cl + O]$^-$ ions as a consequence of oxygen being present, either by atmospheric leakage or by the intentional introduction of the gas. It is still not firmly established if O$_2^-$˙ or O$^-$˙ reacts with the analyte or if M$^-$˙ reacts with O$_2$;[4] however, the latter reaction appears to be more likely. Knighton *et al.*[5] and Stemmler *et al.*[6] have shown that there is a low probability of forming O$_2^-$ from O$_2^-$* by electron attachment. The lifetime of vibrationally excited O$_2^-$* with respect to autodetachment is very short so that collisional stabilization of O$_2^-$* is an inefficient process.

At an ion source temperature of 140 °C and reagent gas source pressure of 0.5 mbar, the ECNI mass spectra of the 24, 3- and 4-MeSO$_2$-, tetrachloro-to heptachloro-MeSO$_2$-PCBs (Table 1) were dominated by M$^-$ (Fig. 2).

The relative abundance of the major fragment ions was <25% (Table 1), indicating that resonance electron capture to form M$^-$ was the favoured anion-forming process. The presence of the major fragment ions, [M − CH$_3$]$^-$, [M − Cl + H]$^-$, [M − CH$_3$ -Cl + H]$^-$, [M − 2Cl]$^-$, [M − 2Cl + 2H]$^-$ and [M − SO$_2$CH$_3$ + H]$^-$, were consistent with the peak assignments described elsewhere;[9,10] however, we suggest a more descriptive notation for the hydrogen inclusion-type ions based on studies found in the literature. Sears *et al.*[7] demonstrated for polyhalogenated unsaturated hydrocarbons that [M − Cl + H]$^-$ and [M − 2Cl]$^-$ are more accurately written as [M + 2H − HCl]$^-$ and [M + 2H − 2HCl]$^-$, respectively, as both originate from an (M + 2H) species formed by the addition of two hydrogen atoms to a double bond of the analyte (sequence 1).[2,25]

$$M \xrightarrow{e^-} M^{*} \longrightarrow M^- $$
$$M \xrightarrow{wall} (M+2H) \xrightarrow{e^-} \begin{cases} (M\text{-Cl+H})^- + HCl \\ (M\text{-2Cl})^- + 2HCl \end{cases} \quad (1)$$

Ion source walls are known to be activated by surface-bound hydrogen atoms generated as a result of e-beam irradiation of the methane buffer gas.[7,26] [M − SO$_2$CH$_3$ + H]$^-$ formation probably follows a similar reaction route originating from (M + 2H), where the fragment ion is more accurately described as [M + 2H − HSO$_2$CH$_3$]$^-$. The formation of [M − 2Cl + 2H]$^-$ ions are thought to originate from [M + 2H − HCl]$^-$ (or [M − Cl + H]$^-$, sequence (1)) by the following reaction:

$$(M\text{-Cl+H})^- \xrightarrow[wall]{P^+} (M\text{-Cl+H}) \xrightarrow{wall} (M\text{-Cl+3H})$$
$$\downarrow e^-$$
$$(M\text{-2Cl+2H})^- + HCl \quad (2)$$

where [M − Cl + H]$^-$ is initially neutralized by positive ion (P$^+$)-electron recombination, followed by catalytic hydrogenation of neutral (M − Cl + H) on the ion source walls. Based on the results of Sears *et al.*,[7] [M − CH$_3$-Cl + H]$^-$ from the MeSO$_2$-PCBs (Fig. 2) probably originates from neutralized [M − CH$_3$]$^-$ following reactions similar to sequence (2).

The most abundant fragment ions, [M − CH$_3$]$^-$ and [M − Cl + H]$^-$, retained the SO$_2$ and MeSO$_2$ functional groups, respectively, suggesting that additional stabilization of the attached electron is afforded by the energically accessible d-orbitals of the sulfur heteroatom. Resonance stabilization and electron sharing, which involves a non-bonding orbital on a heteroatom, are key factors determining the abundance of a product ion, since the presence of heteroatoms can influence fragment ion lifetime in the ion source.[27] The lower abundance of the [M − CH$_3$ − Cl + H]$^-$, [M − 2Cl]$^-$ and [M − 2Cl + 2H]$^-$ fragments, which also retain the SO$_2$ functional group, may be due, in part, to the less facile, multiple bond cleavage necessary for their formation during the dissociative resonance electron-capture process.

The [M − SO$_2$CH$_3$ + H]$^-$ fragment ion was detectable only for the higher chlorinated MeSO$_2$-PCBs

(Table 1), suggesting that greater substitution of electronegative chlorines may be necessary to stabilize the negative charge, and hence lengthen the lifetime of $[M - SO_2CH_3 + H]^-$, which lacks the sulfur-containing moiety. Greater substitution of electronegative chlorine on PCBs is known to enhance negative charge stabilization of fragment ions.[28] Further, the energy necessary to cleave the C—S bond of M^{-*} to form $[M - SO_2CH_3 + H]^-$ probably decreases with increasing substitution of electrophilic chlorine.

Effect of ion source temperature and methane gas pressure on MeSO₂-PCB fragmentation

The effect of increasing the ion source temperature from 100 to 260 °C generally increased the abundance of the MeSO₂-PCB fragment ions relative to M^- (Fig. 3). However, the abundance of all ions decreased with increasing ion source temperature, especially above 200 °C (not shown). An ion source temperature of 140 °C was optimal for the overall enhancement of ion abundance, while facilitating a measurable abundance of fragment ions. A similar ion source temperature effect has been observed for polyhalogenated aromatic hydrocarbons, PCBs and hexachlorocyclopentadiene derivatives.[1,8,22,24] As the ion source temperature is increased, the M^{-*} of halogenated compounds show an increased probability toward a dissociative electron-capture processes at the expense of the non-dissociative electron-capture process.[8,24]

The increase in the relative abundance of the dominant fragment ion $[M - CH_3]^-$ (Table 1) was exponential, increasing sharply above 200 °C (Fig. 3). At still higher temperatures, the abundance of $[M - CH_3]^-$ surpassed that of M^- to become the most abundant ion. The effect of increasing the ion source temperature on the relative abundance of hydrogen inclusion-type ions, $[M - Cl + H]^-$ and $[M - CH_3 - Cl + H]^-$, was not as dramatic as for $[M - CH_3]^-$. The abundance of $[M - Cl + H]^-$ appeared to increase slightly for 3- and 4-MeSO₂-PCBs possessing 2,5-dichloro substitution on the MeSO₂-containing ring (Fig. 3(a) and (b)), whereas for the congeners containing 2,5,6-trichloro substitution (Fig. 3(c) and (d)), the abundance of $[M - Cl + H]^-$ appeared to be independent of ion source temperature. The abundance of $[M - CH_3 - Cl + H]^-$ increased for all MeSO₂-PCB congeners, roughly parallel to the abundance of $[M - CH_3]^-$, at ion source temperatures above 200 °C, to a maximum of ~40% for 3-MeSO₂-2,5,6-trichloro-PCBs (Fig. 3(c)). As mentioned, the formation of hydrogen inclusion-type fragment ions occurs via dissociative electron capture of (M + 2H) created by hydrogenation of the non-ionized analyte on the walls of the ion source, a process which appears to be facilitated by some form of heterogeneous catalysis.[2,7,25] The minimal effect of the change in ion source temperature on the abundance of hydrogen inclusion-type fragment ions as compared with $[M - CH_3]^-$ may be dependent on the rate of ion formation, which is limited by the diffusion of the MeSO₂-PCB analyte to the ion source wall and/or the subsequent heterogenous catalysis on the ion source wall, rather than dissociative processes.
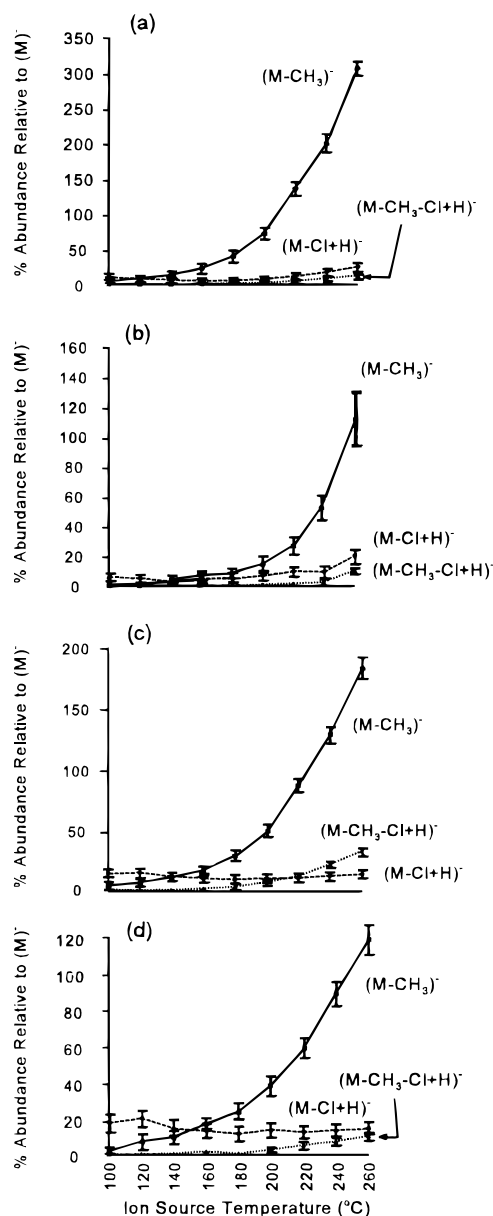
Figure 3. Effect of ion source temperature on the mean abundance of the major fragment ions relative to M^- for MeSO₂-PCB groups possessing the (A) 3-MeSO₂-2,5-dichloro ($n = 6$), (B) 4-MeSO₂-2,5-dichloro ($n = 7$), (C) 3-MeSO₂-2,5,6-trichloro ($n = 5$) and (D) 4-MeSO₂-2,5,6-trichloro ($n = 6$) moiety. See Table 1 for the individual congeners in each set. The standard deviation is represented by error bars. Error bars on points close to zero have been omitted for clarity. The methane gas pressure in the ion source was 0.5 mbar.

These results are consistent with the formation of $[M - X + H]^-$ ions from polyhalogenated unsaturated hydrocarbons, which are not significantly altered by changes in the ion source temperature.[7]
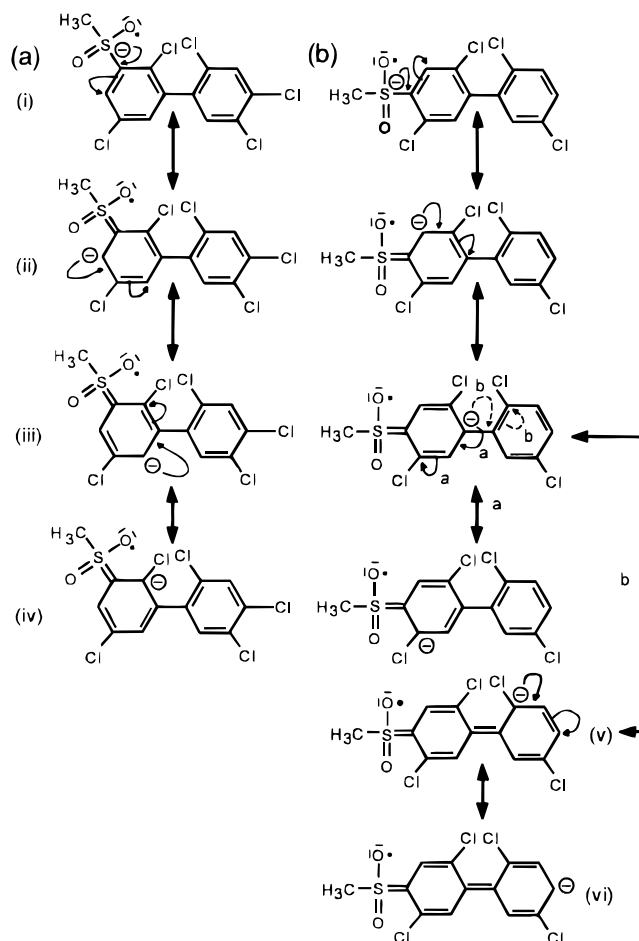
The ratio of $[M - CH_3]^-$ abundance among the ten 3- and 4-MeSO₂-PCB pairs, with each pair possessing the same chlorination substitution pattern, was statistically independent of ion source temperature between 100 and 260 °C (Fig. 4). The temperature range encompassed the 140–200 °C range known to be necessary for optimal electron-capture enhancement of polychlorinated aromatic compounds.[22] The $[M - CH_3]^-$, 3-/4-MeSO₂-PCB abundance ratios were consistently
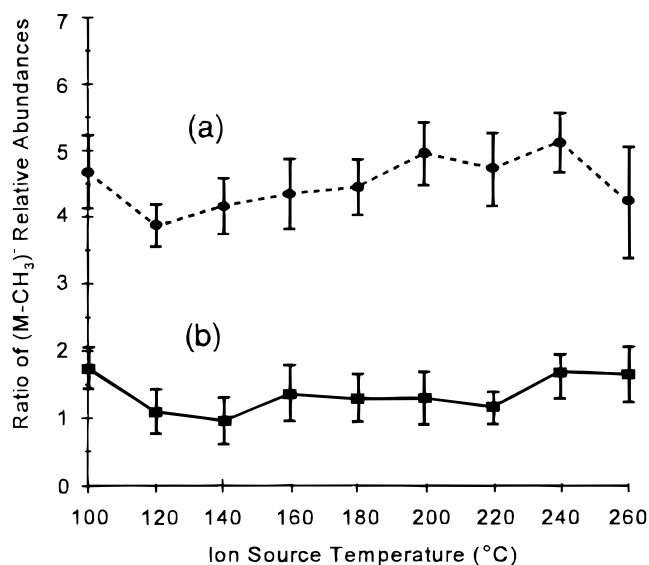
Figure 4. Effect of ion source temperature on the mean ratio of the relative abundance of $[M - CH_3]^-$ between the 3- and 4-MeSO$_2$-PCB pairs possessing the (A) 2,5-dichloro ($n = 6$) and (B) 2,5,6-trichloro ($n = 4$) moieties. The standard deviation among the 3- and 4-MeSO$_2$-PCB pairs (see Table 1) is represented by error bars.

Figure 5. Effect of resonance on the M$^-$ and M$^-$* of (A) 3-and (B) 4-MeSO$_2$-2,2',5,5'-Cl$_6$CB. Note the existence of six as opposed to four canonical structures for the 4-MeSO$_2$-PCB and 3-MeSO$_2$-PCB, respectively. The two lone electron pairs on the radical oxygen are represented by lines. The dotted resonance lines are the change in charge distribution to obtain the canonical structures via path b.

greater than unity and driven by the preference of 4-MeSO$_2$-PCBs to form M$^-$ (Table 1), which may be due, in part, to resonance effects. Two extra canonical structures due to resonance with the second phenyl ring are possible for the M$^-$* of 4-MeSO$_2$-PCB relative to the corresponding 3-MeSO$_2$-PCB pair (Fig. 5). The M$^-$* of the 4-MeSO$_2$-PCB pair is therefore capable of more effective delocalization of the added electron. The M$^-$* of the 4-MeSO$_2$-PCB pair may have a longer lifetime with respect to electron autodetachment, and a greater probability of collisional deactivation to form M$^-$.

The $[M - CH_3]^-$, 3-/4-MeSO$_2$-PCB abundance ratios separated into two distinct congener groups, those MeSO$_2$-PCBs possessing 2,5-dichlorination on the MeSO$_2$-containing phenyl ring with a ratio of ~ 4.5, and congeners with 2,5,6-trichlorination on the same ring with a ratio of ~ 1.5. Stabilization of M$^-$*, and subsequently a greater probability of M$^-$ formation, may be accentuated for congeners possessing a MeSO$_2$-containing phenyl ring with 2,5-dichloro (i.e. one *ortho*-chlorine) as opposed to 2,5,6-trichloro substitution (i.e. two *ortho*-chlorines), where there is less steric interaction between *ortho*-chlorines on the biphenyl system (Fig. 1). Such an interaction between *ortho*-chlorines increases the energy barrier of rotation necessary to achieve a coplanar configuration,[29] and thus reduces the conjugation between the two phenyl rings (Fig. 5). The M$^-$* of the 4-MeSO$_2$-2,5-dichloro-PCBs would therefore be expected to have the longest lifetimes and thus the greatest probability for collisional stabilization to form M$^-$. Alternatively, a plausible explanation for a preference toward $[M - CH_3]^-$ formation for MeSO$_2$-PCB congeners not possessing the 4-MeSO$_2$-2,5-dichloro moiety may be that subtle changes in the activation energy for fragmentation of M$^-$* results in a greater probability of a Frank–Condon transition that leads to an unstable M$^-$*.[4] If such a transition is above the dissociation limit, M$^-$* can undergo a dissociative process.

Reduction of the methane buffer gas pressure from 0.5 to 0.05 mbar resulted in a decrease in the ECNI response sensitivity by an order of magnitude for all MeSO$_2$-PCBs (not shown). This buffer gas pressure effect was consistent with the general finding for chlorinated aromatics that decreasing the gas pressure in the ion source decreases the negative ion abundance.[2] This effect has been attributed to the increase energy in the electron plasma in the ion source and/or a decrease in the probability of the collisional stabilization of M$^-$*.[8] Despite the large difference in sensitivity as a consequence of decreasing the ion source gas pressure, the mass spectra of the MeSO$_2$-PCBs were not significantly altered (not shown). Stemmler and Hites[8] had observed a similar reagent gas pressure effect for the methane ECNI mass spectra of hexachlorocyclopentadiene derivatives.

Lower abundances of $[M - CH_3]^-$ and $[M - Cl + H]^-$ relative to M$^-$ were observed for the 24, 3-and 4-MeSO$_2$-PCBs as compared with a recent study of 12, 3- and 4-MeSO$_2$-PCBs by Buser et al.[9] This may be accounted for by several differences in the GC/ECNI-MS ion source and operating parameters. Buser et al.[9] employed several ECNI-MS parameters different to ours, including a different buffer gas (10% methane–

argon), a much lower ion source pressure $(1.0 \times 10^{-4}$ mbar) and an MS instrument with an ion source differing in physical construction. Depending on the buffer gas used and the nature of the analyte, the molecular ion or fragment ion abundance may be enhanced as the ion source pressure is increased.[2] For example, the ECNI mass spectrum of 1,2,3,4-tetrachlorodibenzo-p-dioxin had a greater abundance of M^- at lower ion source pressures when hydrogen and argon were used as reagent gases, whereas the fragmentation remained unchanged in response to decreasing pressure when helium was used as a reagent gas.[30] The relative importance of resonance and dissociative resonance electron-capture processes is dependent on a complex combination of physical and geometrical parameters of the GC/ECNI-MS instrument, especially for processes involving hydrogen attachment reactions. Therefore, ECNI mass spectra may look completely different under seemingly identical conditions.

Influence of chlorine and $MeSO_2$-substitution on the fragment ion abundance of $MeSO_2$-PCBs

The 2-$MeSO_2$-/2′-Cl-substituted PCBs have been shown to give more complex fragmentation patterns than PCBs with 3- or 4-$MeSO_2$-substitution.[9,10] For the former $MeSO_2$-PCB structures, $[M - CH_3]^-$ and $[M - Cl + H]^-$ tend to dominate the mass spectra whereas M^- is generally $<50\%$ of the fragment ion base peak.[9,10] Therefore, the low abundance of the M^- ion in 2-$MeSO_2$-/2′-Cl-PCBs is currently the primary feature in ECNI mass spectra for structural differentiation among $MeSO_2$-PCBs. The information is of little practical use in environmental analysis since these congeners are not found in biota.[10,11,31] Recent research to determine further correlations between $MeSO_2$-PCB structure and ECNI-MS fragmentation has been inconclusive for two reasons: (i) the $MeSO_2$-PCB product compounds prepared by γ-irradiation of technical PCB mixtures (Aroclor 1254 and 1260) in dimethyl sulfide widely varied in $MeSO_2$- and Cl-substitution pattern, and there were no groups of $MeSO_2$-PCBs that varied in only one structural attribute,[9] or (ii) the presence of molecular oxygen in the ion source overwhelmingly influenced the course of $MeSO_2$-PCB fragmentation.[10] The GC/ECNI-MS system in the present study was devoid of significant O_2 interference. Determining the possible relationships between $MeSO_2$-PCB structure and their fragmentation patterns was also facilitated by the limited variations in the congener structure. All congeners had (i) 3- or 4-$MeSO_2$-substitution, (ii) tetrachloro to heptachloro substitution and (iii) 2,5-dichloro or 2,5,6-trichloro substitution on the $MeSO_2$-containing phenyl ring. These $MeSO_2$-PCB congeners have also been identified as persistent contaminants in biota, including humans.[10–15,31,32]

Differentiation of 3- and 4-$MeSO_2$-PCB structures was suggested by differences in the relative abundance of $[M - CH_3]^-$ (Table 1), where the ion source temperature and buffer gas pressure were 140 °C and 0.5 mbar, respectively. The 4-$MeSO_2$-PCBs tended to have less abundant $[M - CH_3]^-$, regardless of the degree of chlorination, and, as mentioned previously,

was independent of ion source temperature (Fig. 4). Haraguchi et al.[10] had previously observed a slightly greater abundance of $[M - CH_3]^-$ for 3-$MeSO_2$-PCBs, as opposed to 4-$MeSO_2$-PCBs, for congeners with five or more chlorines. The observation was considered qualitative since the mass spectra were obscured by $MeSO_2$-PCB reactions with oxygen. In the present study, the relative abundance of $[M - Cl + H]^-$ tended to be higher for $MeSO_2$-PCBs of greater chlorination. Tetrachloro-$MeSO_2$-PCBs generally had lower levels of the less abundant $[M - CH_3-Cl + H]^-$, $[M - 2Cl + 2H]^-$, $[M - 2Cl]^-$ and $[M - SO_2CH_3 + H]^-$ ions whereas hexachloro-and heptachloro-$MeSO_2$-PCBs had higher relative abundances of the same four fragment ions (Table 1). Additional $MeSO_2$-PCB structure-fragmentation patterns (Table 1) were not obvious from the differences in relative abundances; however, the application of multivariate statistical analysis (PCA) revealed further information.

PC1 and PC2 accounted for 88.6% of the total variance of the abundance among fragment ions and $MeSO_2$-PCB congeners. Figure 6(a) illustrates the scoreplot of PC1 versus PC2 for the 24 $MeSO_2$-PCB
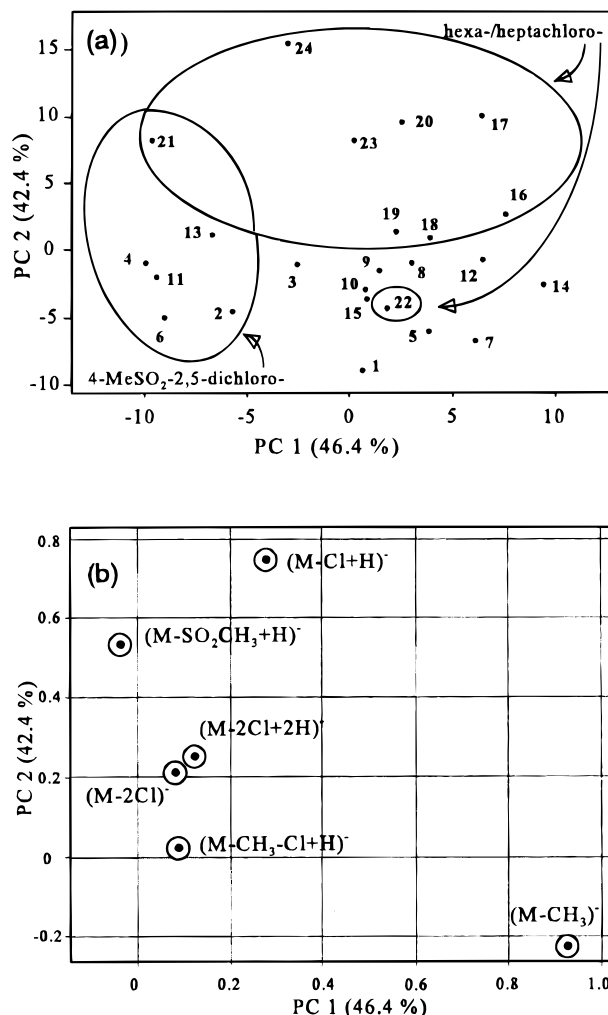
Figure 6. (A) Principal component score and (B) loading plots for the relative abundance of the major ECNI-MS fragment ions for 24 $MeSO_2$-PCBs. See Table 1 for the $MeSO_2$-PCB numbering system. See the Experimental section for a description of the multivariate statistical analysis.

congeners. The PC1 versus PC2 loading plot (Fig. 6(b)) shows how the variation in the relative abundance of the fragment ions influenced the PC1 and PC2 eigenvectors. Ions with the largest influence on a given PC deviate the greatest from zero on the PCA loading plot in the positive or negative direction. Hexachloro-and heptachloro-MeSO$_2$-PCBs had positive PC2 loadings, with the exception of 4-MeSO$_2$-CB151 (point 22, Fig. 6(a)), while less chlorinated congeners had negative loadings. The outlying nature of 4-MeSO$_2$-CB151 may have been due to a lack of a 4'-chlorine (Fig. 1), which was a distinguishing structural feature relative to the other hexachloro-and heptachloro-MeSO$_2$-PCBs. PC2 was driven primarily by the influence of $[M - Cl + H]^-$ (Fig. 6(b)), which tended to have higher relative abundances for the higher chlorinated congeners (Table 1). The $[M - SO_2CH_3 + H]^-$ ion also had a high value along PC2 and higher relative abundances for hexachloro-and heptachloro-MeSO$_2$-PCBs compared with lower chlorinated congeners. The most distinct clustering in the score plot was for MeSO$_2$-PCBs possessing the 4-MeSO$_2$-2,5-dichloro moiety, which had PC1 loadings < -5 (Fig. 6(a)). PC1 was driven almost entirely by $[M - CH_3]^-$ whereas the PC1 values of the remaining ions were close to zero (Fig. 6(b)), and therefore had little modelling power. The MeSO$_2$-PCBs containing the 4-MeSO$_2$-2,5-dichloro moiety all had low relative abundances for $[M - CH_3]^-$, as discussed in the previous section.

CONCLUSIONS

Using pure methane buffer gas and an oxygen-free ion source, $[M - Cl + H]^-$ and $[M - CH_3]^-$ were the most abundant fragment ions in the ECNI mass spectra

of 3- and 4-MeSO$_2$-PCBs (Table 1), and were the most influenced by differences in the position of MeSO$_2$-and chlorine substitution on the biphenyl system. $[M - CH_3]^-$ fragmentation was the most dependent on ion source temperature and pressure. The following ECNI-MS fragmentation rules were elucidated to aid in the identification of unknown 3- and 4-MeSO$_2$-PCB compounds in environmental samples and synthetic products containing isomeric 3-and 4-MeSO$_2$-PCBs:

1. $[M - CH_3]^-$ formation is greater for 3-MeSO$_2$-PCBs relative to the corresponding 4-MeSO$_2$-PCB pair with the same chlorine substitution pattern.
2. The $[M - CH_3]^-$ abundance ratio for the 3-/4-pairs is essentially constant between 100 and 260 °C; however, the ratio is about threefold greater for 3-/4-MeSO$_2$-2,5-dichloro-substituted pairs relative to 3-/4-MeSO$_2$-2,5,6-trichloro-substituted pairs.
3. $[M - Cl + H]^-$ abundance is higher for hexachloro-and heptachloro-MeSO$_2$-PCBs. For the abundance of the hydrogen inclusion-type ions, including $[M - Cl + H]^-$, the ion source temperature is less influential than is observed for $[M - CH_3]^-$ abundance.
4. Relative to more highly chlorinated 3- and 4-MeSO$_2$-PCBs, the tetrachloro congeners tend to have lower abundances of $[M - CH_3 - Cl + H]^-$, $[M - 2Cl + 2H]^-$, $[M - 2Cl]^-$ and $[M - SO_2CH_3 + H]^-$.

REFERENCES

1. B. Arbogast, W. L. Budde, M. Deinzer, R. C. Dougherty, J. Eichelberger, R. D. Foltz, C. C. Grimm, R. A. Hites, C. Sakashita and E. Stemmler, *Org. Mass Spectrom.* **25**, 191 (1990).
2. E. A. Stemmler, R. A. Hites, B. Arbogast, W. L. Budde, M. L. Deinzer, R. C. Dougherty, J. W. Eichelberger, R. L. Foltz, C. Grimm and E. P. Grimsrud, *Anal. Chem.* **60**, 781 (1988).
3. M. Oehme, D. Stockl and H. Knoppel, *Anal. Chem.* **58**, 554 (1986).
4. A. G. Harrison, *Chemical Ionization Mass Spectrometry*, 2nd edn. CRC Press, Boca Raton, FL (1992).
5. W. B. Knighton, J. A. Bognar and E. P. Grimsrud, *J. Mass Spectrom.* **30**, 557 (1995).
6. E. A. Stemmler, J. L. Diener and J. A. Swift, *J. Am. Soc. Mass Spectrom.* **5**, 990 (1994).
7. L. J. Sears, J. A. Campbell and E. P. Grimsrud, *Biomed. Environ. Mass Spectrom.* **14**, 401 (1987).
8. E. A. Stemmler and R. A. Hites, *Anal. Chem.* **57**, 684 (1985).
9. H.-R. Buser, D. R. Zook and C. Rappe, *Anal. Chem.* **64**, 1176 (1992).
10. K. Haraguchi, Å. Bergman, E. Jakobsson and Y. Masuda, *Fresenius J. Anal. Chem.* **347**, 441 (1993).
11. Å. Bergman, R. J. Norstrom, K. Haraguchi, H. Kuroki and P. Béland, *Environ. Toxicol. Chem.* **13**, 121 (1994).
12. K. Haraguchi, M. Athanasiadou, Å. Bergman, L. Hovander and S. Jensen, *Ambio* **21**, 546 (1992).
13. R. J. Letcher, R. J. Norstrom and Å. Bergman, *Sci. Total Environ.* **160/161**, 409 (1995).
14. R. J. Letcher, R. J. Norstrom, S. Lin, M. A. Ramsay and S. M. Bandiera, *Toxicol. Appl. Pharmacol.* **137**, 127 (1996).
15. R. J. Letcher, R. J. Norstrom and Å. Bergman, *Anal. Chem.* **67**, 4155 (1995).
16. R. J. Letcher, R. J. Norstrom and D. C. G. Muir, in *Dioxin'96, Organohalogen Compounds*, edited by K. Olie, Vol. 28, p. 500. Dioxin'96 Secretariat, Amsterdam (1996).
17. J. E. Bakke, Å. L. Bergman and G. L. Larsen, *Science* **217**, 645 (1982).
18. J. E. Bakke and J.-Å. Gustafsson, *Trends Pharmacol. Sci.* **5**, 517 (1984).
19. J. E. Bakke, in *Intermediary Xenobiotic Metabolism in Animals*, edited by D. H. Hutson, J. Caldwell and G. D. Paulson, p. 205. Taylor & Francis, London (1989).
20. K. Haraguchi, H. Kuroki and Y. Masuda, *J. Agric. Food Chem.* **35**, 178 (1987).
21. Å. Bergman, B. Jansson and I. Bamford, *Biomed. Environ. Mass Spectrom.* **7**, 20 (1980).
22. M. Oehme, *Anal. Chem.* **55**, 2290 (1983).
23. R. Guevremont, R. A. Yost and W. D. Jamieson, *Biomed. Environ. Mass Spectrom.* **14**, 435 (1987).
24. F. W. Crow, A. Bjorseth, K. T. Knapp and R. Bennett, *Anal. Chem.* **53**, 619 (1981).

25. S. Erhardt-Zabik, J. T. Watson and M. J. Zabik, *Biomed. Environ. Mass Spectrom.* **19**, 101 (1990).
26. L. J. Sears and E. P. Grimsrud, *Anal. Chem.* **61**, 2523 (1989).
27. F. W. McLafferty, *Interpretation of Mass Spectra*, 3rd edn. University Science Books, Cornell, NY (1980).
28. H. Bagheri, P. E. G. Leonards, R. T. Ghijsen and U. A. T. Brinkman, *Int. J. Environ. Anal. Chem.* **50**, 257 (1993).
29. J. M. Cullen and K. L. E. Kaiser, in *QSAR in Environmental Toxicology*, edited by K. L. E. Kaiser, p. 39. Reidel, Dordrecht (1996).

30. J. A. Lameé, B. C. Arbogast and M. L. Deinzer, *Anal. Chem.* **58**, 2907 (1986).
31. K. Haraguchi, A. Bergman and Y. Masuda, in *Dioxin'94*, *Organohalogen Compounds*, edited by H. Fiedler, Vol. 20, p. 501. Kyoto University Press, Kyoto (1994).
32. K. Haraguchi, H. Kuroki and Y. Masuda, *J. Chromatogr.* **361**, 239 (1986)